SECOND INTERNATIONAL CONFERENCE ON
PORT AND OCEAN ENGINEERING UNDER ARCTIC CONDITIONS
UNIVERSITY OF ICELAND
DEPARTMENT OF ENGINEERING AND SCIENCE

THE WAVE PUMP
APPLICATION IN POLLUTION CONTROL

P. Bruun Professor, Dr.techn.Sc.	The Norwegian Institute of Technology	Trondheim, Norway
G. Viggosson Res. Eng.	Department of Ports and Lighthouses	Reykjavik, Iceland

INTRODUCTION

The wave pump utilizes the momentum of waves breaking on a slope to create a current inside the breaker zone (2, 4, 8). To improve the effectiveness of the wave pump so that even smaller waves may become effective wave heights are beefed up by concentration of wave energy in a funnel. The wave pump therefore consists of the following sections (Fig. 1):

(1) A funnel-shaped entrance

(2) A slope, e.g. an almost buoyant slab which may be raised and lowered by winches or by hydraulic pistons

(3) A discharge-canal which receives its supply of water from the breaking wave. It is an advantage, if this canal widens behind the breaker section.

This paper gives the theoretical background for the wave pump including an alternative solution which includes a curved canal with a sloping section upon which the waves break.

The main application of the wave pump is for pollution control, e.g. on sea coasts where tidal currents are weak while wave action always is available. Tests are in progress in the Icelandic Hydraulic laboratory.

THEORY

The theory upon which the wave pump concept is based is the solitary wave theory combined with longshore current theories. The total volume of water per unit crest length above the still water level is given by (7):

$$Q = 4\ h^2\sqrt{\gamma/3} \qquad (1)$$

h = water depth and $\gamma = H/h$, H = wave height. For the steep slopes which are considered in this paper γ may be put equal to 1.

The energy flux or wave power P in a wave propagating with group velocity C_g in a channel of width W is

$$P = WC_gE \qquad (2)$$

E = energy per unit area of the bottom.

At breaking

$$P_{br} = WC_{gbr}E_{br}$$

The wave power per unit area for a particular wave train may be increased by a gradual decreasing of W thereby concentrating the wave energy. The type of reflection which may occur from the side walls used for concentration of wave energy depends upon the angle of incidence of the waves compared to the alignment of the walls. If the angle between direction of wave propagation and the wall is between 20^0 and 45^0 Mach reflection will occur (3). If the angle is $< 20^0$ it will be no reflection but waves "pile up" along the wall orienting themselves perpendicular to the wall. Wave energy is gradually transferred towards the middle of the funnel from either side. The less the angle of incidence is the smoother and more evenly will said transition take place and the less pile up takes place along the wall.

Consider Fig. 2 which shows a funnel shaped channel of entrance width a with sides deviating α degrees from the direction of wave propagation.

One has:

$$\text{Wave Power } P = W_e C_{ge} E_e = W_x C_x E_x + F_o^x \qquad (3)$$

W_e = width of channel at the entrance = a

W_x = width of channel at point x, $W_x = a - 2(tg\alpha)x$

C_{ge} = group velocity at the entrance

C_{gx} = group velocity at point x

E_e = wave energy per unit width and length at the entrance
$= \frac{1}{8} \rho g H_e^2$

E_x = wave energy per unit area at point x

F_o^x = friction loss (sides and bottom) between x = 0 and x = x

H_e = wave height at the entrance

ρ = density of water

g = acceleration of gravity

x = distance travelled in the direction of wave propagation from the entrance x = 0 to x = x

One has:

$$\frac{dP}{dx} = \frac{d}{dx} (W \cdot C_g \cdot E)$$

At point x:

$$\frac{dP}{dx} = \frac{d}{dx} \left| (a - 2tg\ \alpha \cdot x)(C_g \cdot \frac{1}{8} \rho g\ H^2) \right|$$

$$= C_g \cdot \frac{1}{8} \rho g \left| (a - 2tg\ \alpha \cdot x) 2H \frac{dH}{dx} - 2H^2 \cdot tg\alpha \right|$$

Energy is dissipated by bottom and side friction.
In either case one has for turbulent flow:

$$F \sim H^3$$

which gives:

$$(a - 2tg\ \alpha \cdot x) \cdot 2 \cdot \frac{dH}{dx} - 2H\ tg\alpha \sim H^2 \qquad (4)$$

This equation determines H as function of α, x and friction elements.

Furthermore:

$$W_x \cdot C_{gx} \cdot E_x = W_e \cdot C_{ge} \cdot E_e - F_o^x \qquad (5)$$

where index e refer to the entrance and x to distance from the

entrance.

$$(a - 2tg\ \alpha \cdot x) \cdot C_{gx} E_x = a\ C_{ge} E_e - F_o^x$$

As $C_{gx} = C_{ge}$ for constant depth one has:

$$(a - 2tg\ \alpha \cdot x) \cdot C_g E_x = a\ C_g E_e - F_o^x \tag{6}$$

$$(a - 2tg\ \alpha \cdot x) \cdot C_g \frac{\rho}{8} g H_x^2 = a\ C_g \frac{\rho}{8} g H_e^2 - F_o^x \tag{7}$$

The friction loss is composed of two parts:

$$F_o^x = F_{bottom} + F_{sides} \tag{8}$$

$$F_{\substack{bottom \\ unit\ area \\ unit\ time}} = 2 \frac{1}{T} \int_o^{T/2} \tfrac{1}{2} C_b \rho u^3 dt \tag{9}$$

$$= C_b \frac{(2\pi)^2 \rho}{3} \frac{H^3}{T^3 (\sinh 2\pi h/L)^3}$$

Bottom area = $ax - tg\ \alpha \cdot x^2$ (Fig. 3)

$$F_{\substack{sides \\ unit\ length \\ unit\ time}} = 2 \frac{1}{T} \int_o^{T/2} \int_{-d}^{o} \tfrac{1}{2} \rho C_s |u^3| dt\, dy \tag{10}$$

$$= C_s \frac{\rho\ 4\ w^3}{3\ \pi\ m} (1/3 + \sinh^{-2} mh) H^3$$

$$w = \frac{2\pi}{T} \qquad m = \frac{2\pi}{L}$$

Side area = $h \cdot x / \cos\alpha$

Computing energy losses in time increments T (wave length L_h at depth h) one has:

$$(a - 2tg\ \alpha \cdot x)\ C_{gh} E_x = a\ C_{gh} E_e - F_o^x \tag{11}$$

$$(a - 2tg\ \alpha \cdot L_h) C_{gh} E_x = a\ C_{gh} E_e$$

$$\div \frac{Cs \cdot 4 \cdot \rho \cdot w^3}{3\ \pi\ m} (1/3 + \sinh^{-2} mh) H^3 \frac{L_h \cdot h}{\cos\alpha} T$$

$$\div \frac{Cb\ \rho (2\pi)^2}{3} \frac{H^3}{T^3 (\sinh 2\pi h/L)^3} (aL_h - tg\alpha\ L_h^2) T \tag{12}$$

When energy losses have been determined E_x in eq.(12) may be

computed as:

$$E_x = \frac{1}{8} \rho g H_x^2 \tag{13}$$

$$H_x = \left(\frac{8 E_x}{\rho g}\right)^{\frac{1}{2}} \tag{14}$$

One proceedes then the next wave length until the sloping wall is reached.

As mentioned earlier the inflow of water caused by wave breaking $Q = 4H^2 \sqrt{\gamma/3}$. With respect to the selection of C_b and C_s, C_b may be caused by a more or less rippled sand bottom and probably also by larger irregularities in the sand bottom or it may be caused by a concrete or in any case a more smooth bottom. C_s is the roughness of the concrete wall and may be partly skin friction in the concrete and partly a roughness of a larger order caused by major irregularities in the wall. Tentitatively C_s may be set equal to 0.2. From numereous experiments (e.g. is described in refs. 2 and 7) it is known that the Darcy friction factor f for a rippled sand bottom is approximately 0.1. One has:

$$T = \tfrac{1}{2} \rho C_b v^2 = \frac{\rho g \, v^2 \, f}{8g} \tag{15}$$

or

$C_b = \frac{f}{4} = 0.025$ for predominant flow in one direction as it will occur for waves close to breaking. The most recent laboratory investigation by Tunstall and Inman presented at the Annual Meeting of the American Geophysical Union, 1973, titled "Vortex Formation over Rippled Beds by Progressive Waves" yielded value of $2.0 \cdot 10^{-1}$ for the bottom drag coefficient over rippled bottoms. These waves, however, were much smaller than those we are concerned with in the field. Jonsson (5) found C_b as function of the "amplitude Reynolds Number and the bottom particle amplitude and friction. In our case max velocities always exceed 0.5 m/sec and ripples on the bottom must be in the process of degrading. A C_b value of 0.03, therefore seems to be a better average value.

The tentitative calculations were carried out under simplified assumptions using e.q.(12) and assuming layouts as Fig. 5 with entrance depth d = 1.5 m, length of funnel channel = 60 m, entrance width 30 m and width of wave pump 10 m. With entrance wave heights and periods as indicated in Table 1, one arrived at the figures for

TABLE 1 Computations with $C_b = 0{,}02$, $C_s = 0{,}2$

h	H_e	T	L_0	L	$\tanh\frac{2\pi h}{L}$	$\sinh\frac{2\pi h}{L}$	F_b	F_s	F_b+F_s	$\frac{F_b+F_s}{m^2}$	E_e	E_{60}	H_{br}	H_{br}/L	Q	H_{br}/H_e
m	m	sec	m	m			kgm	kgm	kgm	kgm/m²	kgm/m²	kgm/m²	m		m³/sec	
1.5	0.5	4	25	14.4	0.575	0.703	2740	2250	4990	4.2	31.3	27.1	0.81	0.056	3.8	1.62
1.5	1.0	6	56	22.4	0.400	0.435	27400	19800	47200	39.3	125	85.7	1.44	0.064	7.9	1.44
1.5	1.2	8	100	30.2	0.302	0.317	50220	39000	89220	74.4	180	105.6	1.60	0.053	7.4	1.33
1.5	1.5	10	156	37.9	0.243	0.251	103140	78700	181840	152	280	128.0	1.76	0.046	7.1	1.17

TABLE 2 Computations with $C_b = 0,03$, $C_s = 0,2$

h	H_e	T	L_0	L	$\tanh\frac{2\pi h}{L}$	$\sinh\frac{2\pi h}{L}$	F_b	F_s	F_b+F_s	$\frac{F_b+F_s}{m^2}$	E_e	E_{60}	H_{br}	H_{br}/L	Q	H_{br}/H_e
m	m	sec	m	m			kgm	kgm	kgm	kgm/m^2	kgm/m^2	kgm/m^2	m		m^3/sec	
1.5	0.5	4	25	14.4	0.575	0.703	4104	2250	6354	5.3	31.3	26.0	0.79	0.055	3.6	1.58
1.5	1.0	6	56	22.4	0.400	0.435	41040	19800	60840	50.7	125	74.3	1.34	0.060	6.8	1.34
1.5	1.2	8	100	30.2	0.302	0.317	75240	39000	114240	95.2	180	84.8	1.43	0.047	5.9	1.19
1.5	1.5	10	156	37.9	0.243	0.251	154800	78700	233500	194.6	280	85.4	1.43	0.038	4.7	0.95

TABLE 3 Computations with $C_b = 0{,}07$, $C_s = 0{,}2$

h	H_e	T	L_0	L	$\tanh\frac{2\pi h}{L}$	$\sinh\frac{2\pi h}{L}$	F_b	F_s	F_b+F_s	$\frac{F_b+F_s}{m^2}$	E_e	E_{60}	H_{br}	H_{br}/L	Q	H_e/H_{br}
m	m	sec	m	m			kgm	kgm	kgm	kgm/m²	kgm/m²	kgm/m²	m		m³/sec	
1.5	0.5	4	25	14.4	0.575	0.703	9580	2250	11830	9.9	31.3	21.4	0.72	0.05	3.0	1.44
1.5	1.0	6	56	22.4	0.400	0.435	95760	19800	115560	96.3	125	28.7	0.83	0.037	2.6	0.83
1.5	1.2	8	100	30.2	0.302	0.317	175860	39000	214860	179	180	1.0	0.04	-	-	-
1.5	1.5	10	156	37.9	0.243	0.251	361800	78700	440500	367	280	-	-	-	-	-

discharge in Tables 1 to 3 referring to the situation Fig. 5.

Table 1 assumes a concrete floor $C_b = 0,02$ $C_s = 0,2$

Table 2 assumes a slightly rippled floor, $C_b = 0.03$ $C_s = 0,2$

Table 3 assumes a rippled floor, $C_b = 0.07$ $C_s = 0,2$

The ratio between breaker height and breaker dept (d_b/H_b) can according to available theories (4, 7) hardly exceed one for the horizontal or perhaps slightly sloping (1:50 to 1:100) bottom, but it may exceed one on the slope. From Tables 1, 2 and 3 it may be noted that the smoothest floor gives the best utalization of available wave power. The highly rippled floor (Table 3) seems to decrease wave heights $\geq$ about 1 m (T = 6 sec). Table 1 with $C_b = 0,02$ indicates that waves > 1 m may break before reaching the slope, while $C_b = 0,03$ (Table 2) will carry all wave heights to the slope. This is probably the most realistic case and if tides are negligible the choice of depth at the entrance = 1,5 m = 5 ft seems justified. It is of less importance that the highest waves break before reaching the slope. A distribution of discharge Q as shown in Fig. 4 with dotted line is much to be prefered for the distribution shown with full line. The left part refers to more rapid equalization of wave heights. The quantities in Tables 1, 2 and 3 are useful for comparison and further evaluation. If the number of days with wave heights $\leq$ 0,6 m (2 ft) is high, it is obviously most important to beef up these waves as much as possible even if this may cause loss of momentum for the higher waves.

Table 4 is a practical case from the East Coast of Puerto Rico where waves of 0,5 - 2 ft are by far the most frequent for which reason they first of all should be beefed up.

Table 4 FREQUENCY OF WAVE HEIGHTS AT THE ENTRANCE TO THE FLUSHING CHANNEL

Range of heights	0,5 - 2 ft	2 - 4 ft	4 - 5 ft
Approeimately number of days per year	200	130	35

Fig. 6 shows an alternative solution comprising entrance funnel, parallel side channel and a curved channel with a "beach" installed at the far end causing the waves to break. This solution does not require any operation of a sloping beach, and may be preferable in many cases.

Acknowledgement - The PALMAS DEL MAR COMPANY at Puerto Rico sponsored the research on this project which attempted to develop proper flushing mechanism for their proposed 1,000 boat marina development on the East Coast of Puerto Rico.

LIST OF REFERENCES

1) Bruun, P. and Gerritsen, F., 1960 "Stability of Coastal Inlets", North Holland Publishing Co., Amsterdam

2) Bruun, P., 1963 "Longshore Currents and longshore Troughs", Journal of Geophysical Research, Vol 68 (4), pp 1065-1078

3) Chen, T.C., 1961 "Experimental Study on the Solitary wave Reflection along a straight sloped Wall at oblique Angle of Incidence", Tech.News No 124 Beach Erosion Beach, U.S. Army Corps of Engineers

4) Galvin, Cyril Jr., 1967, "Longshore current velocity. A review of theory and data" Review of Geophysics Vol 5 (3) pp 287-303

5) Jonsson, I., 1966 "Wave Boundary Layers and Friction Factors", Proc. 10th Conference in Coasted Engineering Chapter 10

6) Le Méhauté, B., 1961 "Submerged Breakwater for silt Deposition Reduction", Civil Engineering Report No 20, Queens University at Kingston, Ontario, Canada

7) Munk, W.H., 1949 "The solitary wave theory and its application to surf problems", Ann. N.Y. Acad. Sa, Vol 5, pp 376-424

8) Putnam,J.A., W.H. Munk and M.A. Traylor, 1949 "The prediction of longshore currents", Trans. Amer. Geophys. Union, Vol 30, pp 337-345

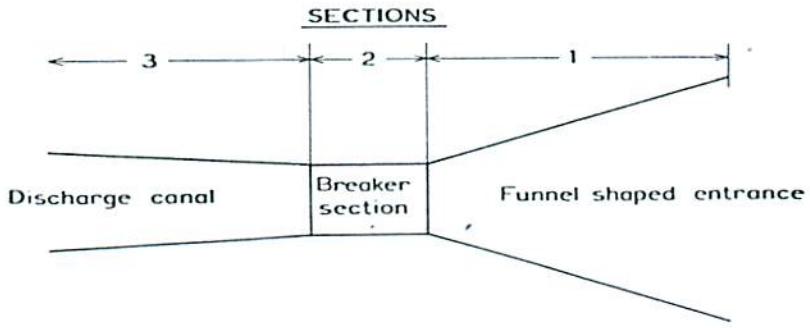

Fig. 1. Wave Pump, Schematics

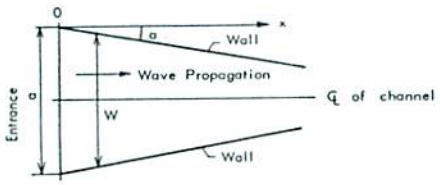

Fig. 2. Funnel Geometry

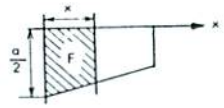

Fig. 3. Bottom area of funnel

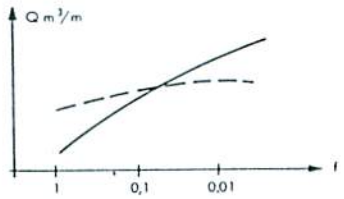

Fig. 4. Discharge versus frequency of occurence. Full line refer to all waves. Dotted lines refer to waves which break

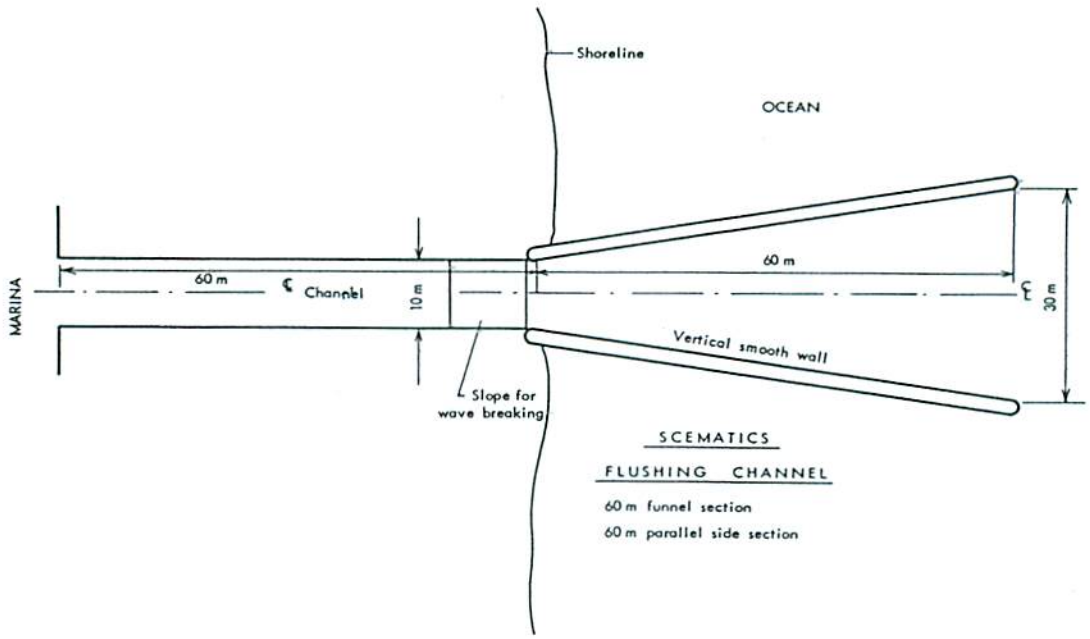

Fig. 5. Wave pump with straight discharge channel. Waves break on slope

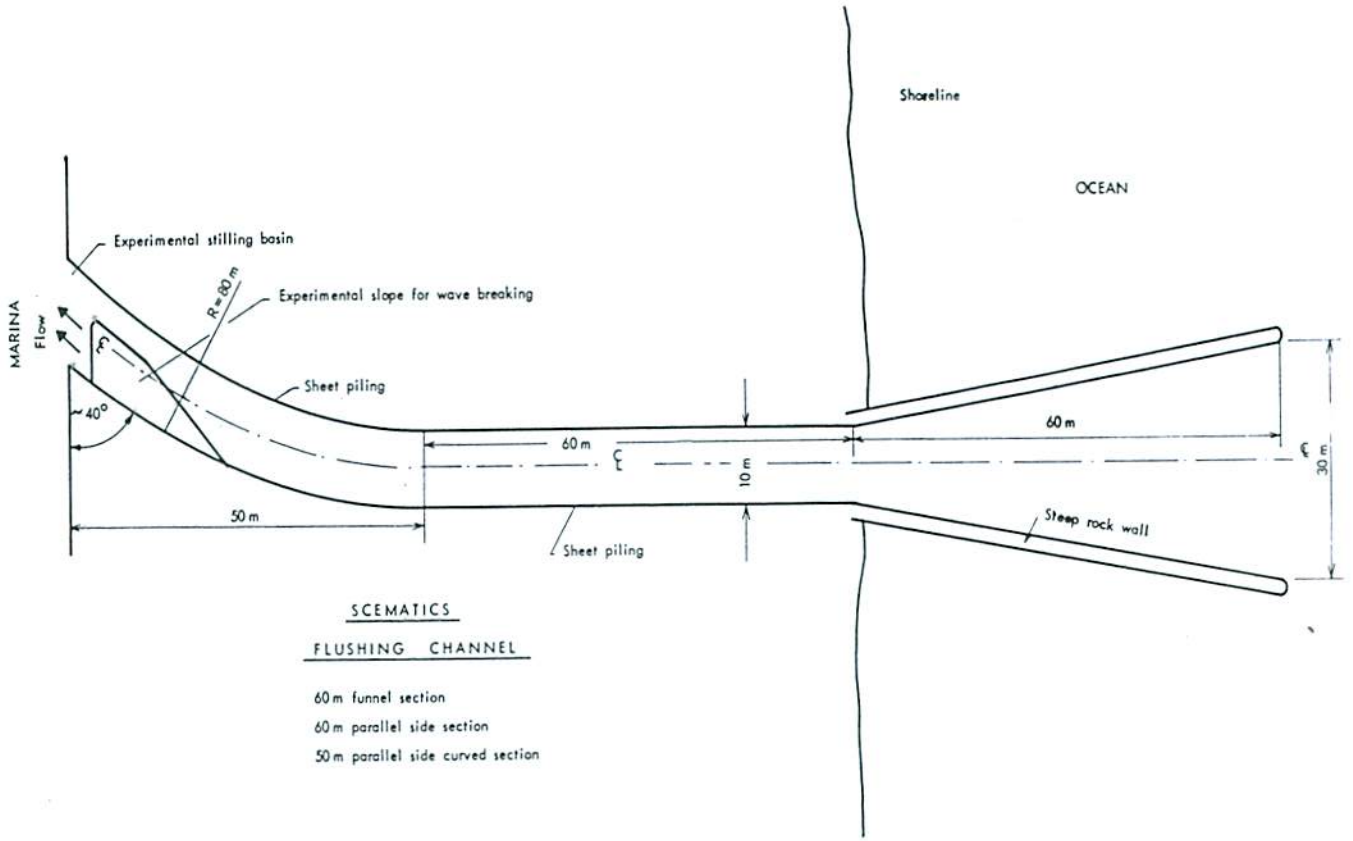

Fig. 6. Wave pump with curved discharge channel in which waves break